THE JOURNAL OF COMPARATIVE NEUROLOGY 376:128–142 (1996)

The Actin Network in the Ciliary Stalk of Photoreceptors Functions in the Generation of New Outer Segment Discs

IRENE L. HALE, STEVEN K. FISHER, AND BRIAN MATSUMOTO
Neuroscience Research Institute and Department of Biological Sciences, University of California, Santa Barbara, California 93106

ABSTRACT

Cytochalasin D (CD) interferes with the morphogenesis of outer segment disc membrane in photoreceptors. Disruption of either the actin network in the ciliary stalk, where membrane evagination is initiated, or the actin core of the calycal processes, whose position could define the disc perimeter, could be responsible. We have attempted to determine which of these local F-actin populations is involved in membrane morphogenesis and what step in the process is actin-dependent. Biocytin accumulation in nascent discs, detected by fluorescent avidin and laser scanning confocal microscopy (LSCM), provided a means of labeling abnormal discs and a measure of disc membrane addition. F-actin content and distribution were assessed using fluorescent phalloidin and LSCM. First, we examined the effects of a range of CD dosages (0.1, 1.0, or 10.0 μM) on rod photoreceptors in *Xenopus laevis* eyecup cultures. Ectopic outgrowth of discs, evaluated by LSCM and transmission electron microscopy (TEM), occurred at each concentration. Phalloidin labeling intensified in the ciliary stalk with increasing CD concentration, indicating F-actin aggregation. In contrast, it diminished in the calycal processes, indicating dispersal; TEM showed that calycal process collapse ensued. Disruption was evident at a lower concentration in the ciliary stalk (0.1 μM) than in the calycal processes (1.0 μM). TEM confirmed that the calycal processes remained intact at 0.1 μM. Thus, CD's action on the ciliary stalk network is sufficient to disrupt disc morphogenesis. Second, we examined the effect of CD on temperature-induced acceleration of the rate of disc formation. In the absence of CD, a 10°C temperature shift increased the disc formation rate nearly three-fold. CD (5 μM) caused a 94% inhibition ($P < 0.025$) of this response; yet, the rate of membrane addition to ectopically growing discs exhibited the expected three-fold increase. Thus, CD's action interferes with the generation of new discs.

Indexing terms: cytoskeleton, cytochalasin D, morphogenesis, morphology, confocal

Photoreceptor outer segment (OS) disc morphogenesis is a highly specialized kind of nonmuscle cell motility involving membrane protrusion and expansion (Steinberg et al., 1980) in which microfilaments have been shown to play a role (Williams et al., 1988). Other well-known examples include formation of the acrosomal process in sperm and extension of lamellipodia and filopodia in translocating cells and neuronal growth cones. Cytochalasin, which blocks actin filament elongation (Sampath and Pollard, 1991) and disorganizes the actin cytoskeleton (reviewed by Cooper, 1987), inhibits motility in these systems (Wessells et al., 1971; Tilney and Inoué, 1982; Marsh and Letourneau, 1984). The light-sensitive OS of vertebrate photoreceptors is a modified cilium. Its photopigment-containing membranes are an elaboration of the ciliary membrane to form discs organized in a stack and contained within, but separate from, the plasma membrane. The double-sided discs arise by evagination of the ciliary membrane at the distal ciliary stalk (Steinberg et al., 1980; Williams et al., 1988). New discs are formed throughout life at this site, where the ciliary stalk joins the base of the OS (Young and Droz, 1968). Continual addition is balanced by loss from the distal tip (Young and Bok, 1969). Hence, knowledge of the mechanism by which discs are formed and of its regulation is important to understand how photoreceptor differentiation and OS membrane renewal are controlled. In addition, this knowledge, as it relates to actin's role, may provide general insight into actin-based motility and the local determination of cell shape.

Accepted May 7, 1996.

Address reprint requests to Brian Matsumoto, Neuroscience Research Institute, University of California, Santa Barbara, CA 93106.

Actin has been localized to two sites that could be important in the mechanism of disc morphogenesis: the distal ciliary stalk, at the site of membrane evagination, and the calycal processes, which resemble microvilli and project from the inner segment (IS) alongside the base of the OS (diagrammed in Fig. 1A; Drenckhahn and Groschel-Stewart, 1977; Burnside, 1978; Chaitin et al., 1984; Chaitin and Bok, 1986). Fluorescent phalloidin, a probe specific for filamentous actin (F-actin; Wulf et al., 1979), stains both of these locations (Drenckhahn and Wagner, 1985; Nagle et al., 1986; Vaughan and Fisher, 1987). Williams et al. (1988) tested the effects of cytochalasin D (CD) on the photoreceptor actin cytoskeleton and on disc formation by using frog eyecups as an experimental system. After treatment with 5 μM or 25 μM CD, phalloidin labeling was faint or absent in both the calycal processes and the ciliary stalk, indicating disassembly or dispersal of actin filaments, and disc membrane formation was abnormal. The most basal discs grew out alongside the OS or IS, greatly exceeding their normal diameter (diagrammed in Fig. 1B). Vaughan et al. (1989) extended these observations to rabbits in vivo.

Williams et al. (1988) proposed two mechanisms by which disruption of the local actin cytoskeleton could result in ectopic disc outgrowth. Either or both of these mechanisms could be operating. First, if the calycal processes act as a signal to terminate outgrowth, then loss of the actin core and their resultant collapse would remove the control of disc diameter. Second, if F-actin in the ciliary stalk is involved in the initiation of membrane evagination, then disruption of this network would inhibit new disc formation. Membrane components would continue to be added to immature discs, those that are already initiated but not fully sealed by rim formation. Excessive growth would result from continued disc expansion outpacing rim closure. In fact, these investigators observed continued incorporation of radiolabeled membrane components into the few ectopic discs.

To understand how actin filaments participate in photoreceptor disc morphogenesis, we have attempted to distinguish between these two models. Two strategies were used. First, we tested whether the ciliary stalk actin network and the calycal process F-actin core are differentially sensitive to CD, and then determined if a dose that affects only the most sensitive F-actin array is sufficient to cause excessive disc growth. If so, that component of the actin cytoskeleton would be implicated in the mechanism of disc morphogenesis. Comparison of the doses at which cytochalasin produces different effects shows that at least a 2.5- to 10-fold higher concentration is necessary to cause contraction of stress fibers and cell retraction than to disrupt leading edge actin network structure and motility (Yahara et al., 1982 and references therein; Lankford and Letourneau, 1991; Kolega et al., 1991). The F-actin core of epithelial cell microvilli is even more stable. In most cases, a 20- to 100-fold higher concentration does not cause dissolution of the core and microvillar collapse (Wrenn and Wessells, 1970; Burgess and Grey, 1974; Madara et al., 1986). In a direct comparison, Yahara et al. (1982) found that CD inhibited membrane ruffling in fibroblasts at 0.2 μM, but caused stress fiber contraction at 2 μM or higher. At 20 μM CD, microvilli and their F-actin core have been found to remain intact in epithelial cells of intestine (Madara et al., 1986) but not differentiating oviduct (Boisvieux-Ulrich et al., 1990). In both cell types, the terminal web of actin filaments was disrupted at this dose. In photoreceptors, actin filaments in the ciliary stalk are organized as a network (Arikawa and Williams, 1989; Chaitin and Burnside, 1989), whereas the core of actin filaments in the calycal processes resembles that of epithelial microvilli (Burnside, 1978; O'Connor and Burnside, 1981) and, hence, may exhibit similarly high stability.

Second, to investigate which step in the disc morphogenesis process is blocked by CD, we varied the disc formation rate. When the ambient temperature is elevated to accelerate metabolism in frogs, the rate of disc formation, measured as disc displacement, increases approximately 2- to 3.5-fold for a 10°C rise in temperature (Hollyfield et al., 1977; Hollyfield, 1979; Hollyfield and Rayborn, 1982). If CD directly inhibits the initiation of membrane evagination, then raising the temperature (which increases the disc formation rate in the absence of the drug) should cause no increase when CD is present. However, if CD interferes with the control of disc diameter, at least a partial increase should be observed.

Both experimental strategies provided evidence to support the model in which the actin network in the ciliary stalk functions in the initiation of ciliary membrane evagination. The results suggest a link between a specific structural effect of CD, disruption of the ciliary actin network, and its functional effect on disc morphogenesis. We discuss different functional effects that could result in the block of new disc initiation.

Abbreviations

CD	cytochalasin D
IS	inner segment
LSCM	laser scanning confocal microscopy
OS	outer segment
TEM	transmission electron microscopy

MATERIALS AND METHODS

Preparation and culture of eyecups

We used a frog eyecup culture system to allow precise control of external drug concentration, as described by Williams et al. (1988). Postmetamorphic *Xenopus laevis* (Charles Sullivan, Nashville, TN) were kept for at least 1 month on a 12-hour alternating light-dark cycle at 20–21°C. The frogs were handled according to the guidelines of the Animal Care Council of the University of California, Santa Barbara. The frogs were killed by decapitation without prior anesthesia 3 to 4 hours after light onset. The eyes were removed and prepared for culture by dissecting away the anterior segments, including cornea, iris, and lens, to form eyecups consisting of the neural retina-retinal pigment epithelium supported by the sclera (Besharse and Dunis, 1983). In one experiment, isolated neural retinas were used to expose the photoreceptors directly to the medium. They were gently peeled away from the retinal pigment epithelium and removed from the eyecup.

The eyecups or isolated retinas were incubated in small, stoppered flasks in Wolf and Quimby (GIBCO, Grand Island, NY) amphibian culture medium (W&Q medium), which was supplemented with $NaHCO_3$ (35 mM, final concentration; Besharse and Dunis, 1983) and gassed continuously with humidified 95% O_2 and 5% CO_2. The flasks were kept on a rotator (50 rpm) to stir the medium gently. The eyecups initially were placed in W&Q medium at 23–24°C and then were treated as follows.

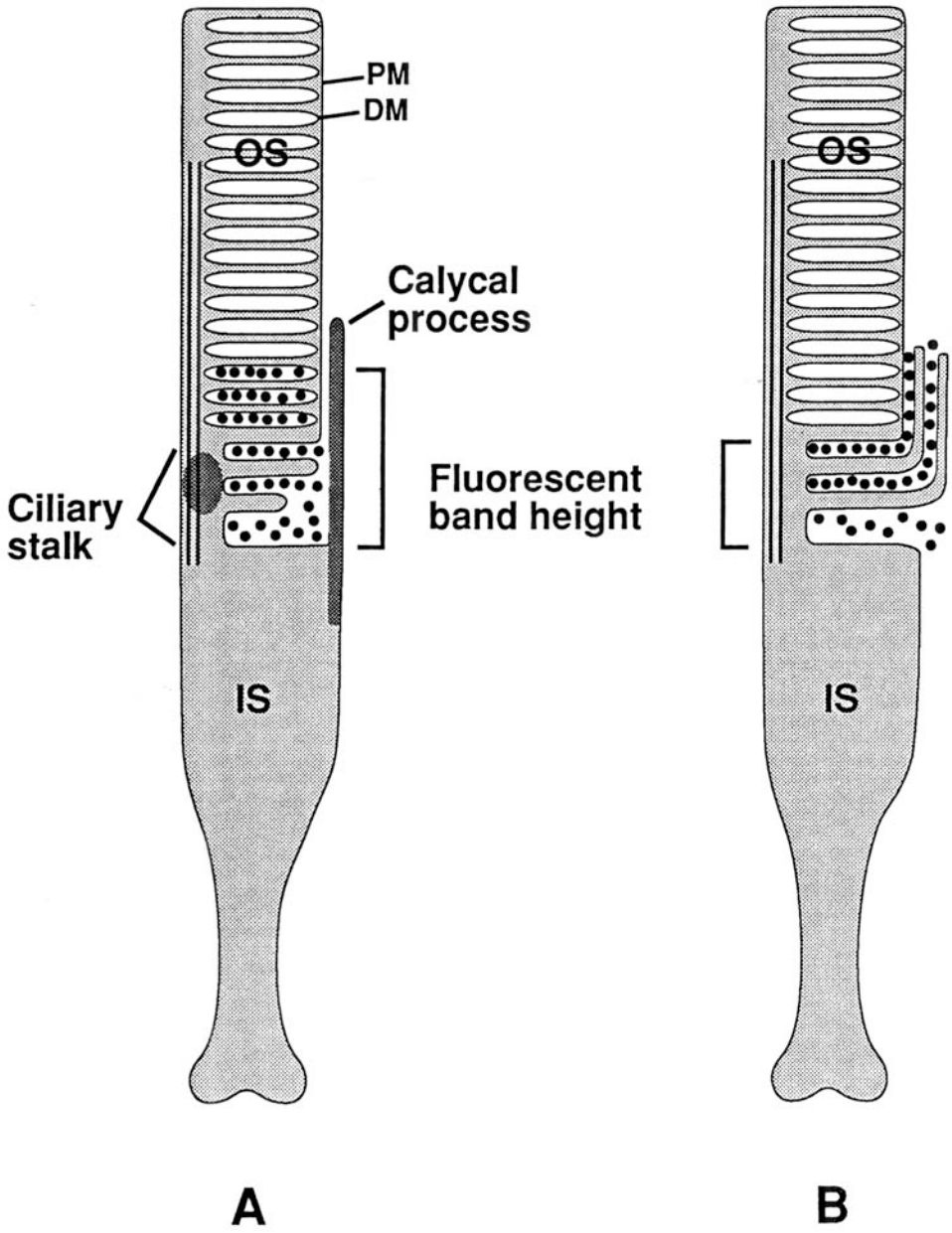

Fig. 1. Diagram of photoreceptor phalloidin labeling and rod outer segment (OS) disc labeling with biocytin. (**A**) Normal frog photoreceptor shown in longitudinal section. Dark stippling represents fluorescent phalloidin labeling of F-actin in the ciliary stalk and of one of the calycal process actin cables. As ciliary membrane evaginations grow laterally to form the disc faces, the future intradiscal space initially is exposed to the extracellular medium. A second outgrowth of membrane around the disc periphery then seals this space. Consequently, discs formed during incubation in biocytin are filled with this tracer (dots). After fluorescent avidin detection, they appear in longitudinal section as a band of fluorescence at the base of the OS (see Fig. 6A,B). The height of this band increases with incubation time as a result of continual disc initiation and distal displacement. (**B**) Cytochalasin (CD)-treated rod photoreceptor. After the same incubation period, the fluorescent band height is decreased because CD slows the rate of disc initiation. Assembly of disc membrane continues, extending the immature discs beyond their normal diameter. These ectopic discs are filled with biocytin and appear as a fluorescent sheet after fluorescent avidin detection (see Fig. 6E,F). OS, outer segment; IS, inner segment; PM, plasma membrane; DM, disc membrane.

Treatment with varied concentrations of CD

CD (Calbiochem, San Diego, CA) was dissolved in dimethyl sulfoxide (DMSO) to give a 10 mM CD stock solution, which was diluted serially to give a final CD concentration in the culture medium of either 10.0, 1.0, or 0.1 μM. The final DMSO concentration was 0.1% in all cases. Medium containing 0.1% DMSO served as a control. After the eyecups were collected in W&Q medium, they were transferred to CD or DMSO medium and incubated for 6 hours at 23–24°C. At the end of the incubation period, additional, freshly dissected eyecups were collected to serve as untreated controls.

Left and right eyes of the same animal were divided between CD and DMSO or between different CD doses for comparison. Four to six eyecups—two or three each for fluorescence microscopy or transmission electron microscopy (TEM)—were used for each treatment, and three replicate experiments were performed. In two experiments, the tracer, biocytin, was added to the medium to monitor ectopic growth of disc membranes (see below). In addition, in two experiments, the short-term effects of CD were investigated. Two eyecups for each dose were incubated for only 2 hours.

Treatment with 5 μM CD at varied temperatures

To achieve a constant pH across the range of temperatures, the pH of the culture medium (7.4–7.6) was adjusted by adding sterile 1N NaOH (Sigma, St. Louis, MO) to 17°C medium or 1N HCl to 27°C medium. When eyecups were shifted to a new temperature, they were transferred with a gradual exchange to fresh medium at the proper temperature and pH. After the eyecups were collected in W&Q medium at 23–24°C, they were transferred to 17°C for 2.5 hours to equilibrate to the lower temperature. Then they were transferred to medium containing 5 μM CD and 0.1% DMSO or DMSO alone along with the tracer, biocytin (see next section), at 17°C for 2.5 hours. This duration is sufficient for the drug to affect the actin cytoskeleton and for small tracer molecules to reach the interphotoreceptor matrix surrounding the photoreceptor OS (Vaughan et al., 1989). At this point, half the eyecups were transferred to 27°C, still with CD or DMSO and biocytin. The eyecups were incubated at 17°C and 27°C in the continuous presence of the drug and the tracer for 12 hours. The lights were kept on through the normal dark period of the lighting cycle to maximize membrane assembly (Besharse, 1980).

Left and right eyes of each animal were divided between drug and control media or between temperatures for comparison. Four eyecups per treatment were used, and two replicate experiments were performed. Eyecups were examined by fluorescence microscopy.

Fluorescent band height assay for disc addition

Immature rod OS discs can be labeled with dyes or other small tracers as described by Laties et al. (1976), Kaplan et al. (1982), and Matsumoto and Besharse (1985). Biocytin (Molecular Probes, Eugene, OR), a biotin-lysine conjugate, was used to label both normal and ectopic discs formed during the incubation period (diagrammed in Fig. 1). This tracer was chosen because it does not bind to OS membranes but can be fixed in place with glutaraldehyde; molecules that bind can cause disorganized stacking of new discs (Vaughan et al., 1989). Biocytin was added to the culture medium to give a final concentration of 0.1%.

Electron microscopy

Eyecups were fixed for 1.5 hours on ice in 1.65% glutaraldehyde/1% osmium tetraoxide in 0.1M sodium cacodylate buffer, pH 7.3. Next, they were rinsed in water, en bloc stained in 1% uranyl acetate in water for 30 minutes, and rinsed in water again. Finally, they were dehydrated in acidified 2,2-dimethoxypropane for 10 minutes (Muller and Jacks, 1975) and embedded in Spurr's resin (Spurr, 1969). Ultrathin sections were cut and stained with uranyl acetate and lead citrate. For counting the number of calycal processes and evaluating calycal process ultrastructure and disc overgrowth, blind observations of 15–20 rods in cross-section per retina were made. Only data from the larger diameter, red rods was used.

Histochemistry

The procedure has been described in detail elsewhere (Hale and Matsumoto, 1993; Matsumoto and Hale, 1993). Briefly, eyecups or isolated retinas were rinsed in an F-actin stabilizing buffer: 100 mM PIPES, 25 mM HEPES, 15 mM EGTA, and 2 mM $MgCl_2$, pH 6.9 with KOH (Edmonds and Koenig, 1990; modified from Schliwa and van Blerkom, 1981). Next, they were fixed in chilled 0.1% glutaraldehyde/4% paraformaldehyde in the same buffer for 30 minutes, followed by 4% paraformaldehyde at 4°C overnight. After fixation, tissues were rinsed in the F-actin stabilizing buffer, followed by phosphate-buffered saline (PBS), pH 7.3; reduced in 0.1% sodium borohydride in PBS, pH 8.0; and rinsed further in PBS, pH 7.3. Thick sections (75–100 μm) of the retina supported in a matrix of 5% agarose (low gelling temperature; Type XI, Sigma, St. Louis, MO) in PBS were cut on a Vibratome (Model 1000, Technical Products International, Kansas City, MO). Retinal sections were incubated free-floating, and solutions were gently stirred on a rotator during incubations and rinses. Equal numbers of sections per volume were incubated in 10 units/ml rhodamine- or fluorescein-conjugated phalloidin (Molecular Probes, Eugene, OR) in PBS, pH 7.3, containing 0.1% Triton X-100 (PBS/Triton) at 4°C for 3–4 hours. Then sections were rinsed in PBS/Triton at 4°C for several hours and mounted in a fluorescence preservative solution of 5% *n*-propyl gallate in glycerol. The phalloidin concentration was approximately saturating, based on qualitative observation. A series of concentrations was tested on sections from both DMSO- and CD-treated (10 μM) retinas. Labeling intensity was diminished at 2 units/ml and unchanged at 20 units/ml, compared with that at 10 units/ml.

To detect biocytin labeling, retinal sections were stained with fluorescent avidin. Sections were incubated in a 5 μg/ml solution of either Cy3-conjugated streptavidin (Jackson ImmunoResearch, West Grove, PA) or fluorescein-conjugated UltraAvidin (Leinco Technologies, St. Louis, MO) in PBS, pH 7.3, containing 1% bovine serum albumin and 0.1% Triton X-100 (PBS/BSA/Triton) at 4°C for 16–18 hours. Sections were rinsed in the same buffer and mounted as above.

For tubulin immunohistochemistry, sections previously stained with fluorescein-phalloidin were incubated in a solution of normal goat serum diluted 1/50 in PBS/BSA/Triton at 4°C for 2 hours. The PBS/BSA/Triton buffer was used for all incubations and rinses. After rinsing, sections then were incubated in a 1/1000 dilution of a monoclonal antibody to β-tubulin, antibody E7 (Chu and Klymkowsky, 1989), at 4°C for 20–24 hours. They were rinsed and then incubated in a solution of 50 μg/ml rhodamine-conjugated, affinity purified goat anti-mouse immunoglobulin G antibody (Cappel Research Products, Organon Teknika Corp., Durham, NC) at 4°C for 18–20 hours. After antibody labeling, sections were rinsed and mounted as above.

Fluorescence confocal microscopy and image analysis

Photoreceptors were viewed with either a Bio-Rad MRC-500 point scanning (Bio-Rad Microsciences, Cambridge, MA) or a Meridian InSIGHT PLUS direct view (Meridian

Instruments, Okemos, MI) laser scanning confocal microscope (LSCM). Optical section thickness was approximately 0.5–0.75 μm. Images were acquired on the Bio-Rad system with a photomultiplier tube and on the Meridian system with either a cooled, charged coupled device (CCD) camera (Optronics TEC-470, Optronics Engineering, Santa Barbara, CA) for qualitative evaluation or a silicon intensified target (SIT) camera (DAGE 66, DAGE-MTI, Michigan City, IN) for quantitative work. Images from the Meridian system were recorded onto high-resolution videotape and subsequently digitized with a TARGA-M8 frame grabber (Tru-vision). Double-label images were collected on the Bio-Rad system using two detectors.

To ensure accurate comparisons of intensity and size, the SIT camera gain, contrast, and black levels were set so that pixel intensities for structures of interest were below the maximum value and above the dark current and tissue autofluorescence values. In addition, rhodamine-phalloidin–labeled retinas were analyzed as sets: images of one control and one retina from each treatment were collected during a single session at constant settings, including confocal aperture size, laser power, and camera settings. Settings were similar between sessions but cannot be reproduced exactly. The SIT camera response was linear over the three log units of intensity measured. Image magnification was chosen so that the dimensions of the structures of interest were several times greater than the pixel size. Image enhancement for quantitation involved only averaging 128 frames using a Hamamatsu DV 3000 image processor (Waltham, MA) to reduce noise.

Rhodamine-phalloidin labeling in the ciliary stalk was quantified on digitized images using interactive image analysis software (JAVA, Jandel Scientific, Corte Madera, CA). The fluorescent region was outlined, and the area and density (average intensity per unit area) were calculated. To avoid shading artifacts from overlying material, optical sections were collected only within a 3- to 4-μm depth from the section surface facing the objective lens. Blind observations of 20 longitudinally oriented rod photoreceptors from each retina were made. Length measurements were made using the Hamamatsu image processor. The height of the band of biocytin plus fluorescent avidin labeling was measured in images collected near the center of the ROS base, whereas the length (extent along rod cell long axis) and width (1-D estimate of extent around circumference) of the sheet of ectopic membranes were measured in images collected at the cell surface. Blind observations of 30 longitudinally oriented rod photoreceptors from each retina were made. For CD-treated photoreceptors, fluorescent band height was measured only in rods that displayed an obvious drug response, that is, that had visible ectopic disc membranes. For calculating the percentage of rod photoreceptors with abnormal OS disc membranes and counting the number of calycal processes that contained F-actin, blind observations of 30 rods in cross-section per retina were made. For double-label examination of ectopic membrane sheets and phalloidin labeling, blind observations of 15–20 rods in cross-section per retina were made. Only data from the larger diameter, red rods were used.

For photographic output, image enhancement included averaging 64–128 frames to reduce noise and remapping the intensity scale to expand the mid-range and/or increase the contrast. Images were printed on a Kodak XL7700 dye sublimation printer (New York, NY).

RESULTS

Dose response

A range of CD concentrations—0.1, 1.0, and 10.0 μM—was tested to look for a difference in sensitivity to the drug between the actin network in the ciliary stalk and the actin bundles in the calycal processes. The effect of these concentrations on disc membrane morphogenesis was assessed to establish the effective doses for comparison to the effects on the actin cytoskeleton.

Effect of CD on membrane morphogenesis

CD disrupted OS disc morphogenesis in rod photoreceptors at all concentrations tested. No abnormal disc outgrowth was evident in DMSO-treated control retinas. After 6 hours in the presence of the drug, ectopic discs labeled with biocytin plus fluorescent avidin (diagrammed in Fig. 1B) appeared as a sheet extending along the OS, IS, or both. When viewed by TEM, the sheet was composed of a stack of approximately seven discs on average. This effect of CD on disc morphogenesis is the same as that found by Williams et al. (1988) and Vaughan and Fisher (1989). The only obvious difference among different CD dosages was an increase in the percentage of rods exhibiting ectopic membranes with increasing CD concentration. These percentages from fluorescence LSCM observations were 21%, 70%, and 93% at 0.1, 1.0, and 10.0 μM CD, respectively.

Effect of CD on actin filament organization

In both untreated and DMSO-treated retinas, the pattern of fluorescent phalloidin labeling (Figs. 2A, 3A) matched that previously described for photoreceptor cells by other investigators (Drenckhahn and Wagner, 1985; Nagle et al., 1986; Vaughan and Fisher, 1987). Calycal process-IS actin cables were visible by fluorescence LSCM as intense lines of fluorescence. F-actin networks visible as more diffuse labeling, along with some smaller fibers, were spread throughout the rest of the IS and the cell body. The synaptic terminal was difficult to distinguish from other elements in the plexiform layer. The actin network in the ciliary stalk appeared as a small spot of fluorescence at the base of the OS, which colocalized with the ciliary microtubules (Fig. 2A).

CD disrupted the actin cytoskeleton in a complex, dose-dependent manner. Its effects were manifested in two main ways: 1) the loss of F-actin from the calycal processes and the areas normally occupied by the IS cables and the IS and cell body networks, and 2) the aggregation of F-actin at various locations, including the ciliary stalk. The effects were most severe in retinas treated with 10 μM CD. At this dose, almost no phalloidin labeling of calycal process-IS cables could be detected (Fig. 2B). This result is in agreement with the nearly complete disassembly or dispersal of F-actin in response to 5 and 25 μM CD reported by Williams et al. (1988). However, we observed a different response in other parts of the cell. The normally diffuse IS labeling was replaced by bright, punctate labeling, as was cell body labeling, and the spot in the ciliary stalk became more prominent (Fig. 2B), indicating focal concentration of F-actin in these regions rather than its complete loss. This response resembled the cytochalasin-induced formation of brightly staining F-actin aggregates seen, for example, in fibroblasts (Weber et al., 1976) and in other neuronal cell types (Marsh and Letourneau, 1984; Edmonds and Koenig, 1990).

At the light microscope level, the two actin filament populations of interest, the ciliary stalk network and the calycal process core, showed differential sensitivity to CD. After exposure to 0.1 μM CD for 2 hours, phalloidin labeling in the ciliary stalk was more intense than normal, whereas labeling in the calycal processes was not noticeably different based on qualitative examination. Even after 6 hours (Fig. 3B), calycal process labeling intensity was unchanged, although in some preparations, the processes were elongated. No obvious changes in phalloidin labeling were observed in the IS at 0.1 μM CD. The ciliary labeling increased in intensity with CD concentration (Fig. 3C,D). Quantitation of the fluorescent signal at this site after 2 hours of drug exposure revealed that a small increase in density and mainly an increase in area contributed to the increase in mean total intensity (Fig. 4). Because measurements were performed on a two-dimensional image, the increase in area represents an increase in volume. The percent increase in total intensity relative to DMSO-treated controls progressed from 95% at 0.1 μM to 140% at 1.0 μM and 315% at 10.0 μM CD. These increases were significant at the 5% level (0.1 and 1.0 μM) or below (10.0 μM, $P < 0.01$), when evaluated by the Student's t-test. The shape of this concentration of fluorescence also changed. From primarily spherical in DMSO-treated rods, it became ovoid at 0.1 and 1.0 μM CD and somewhat irregular at 10.0 μM (Figs. 2, 3).

In addition to overall calycal process phalloidin labeling intensity, the average number of calycal processes per cell counted by fluorescence LSCM also was normal at 0.1 μM CD. Rod photoreceptors treated with DMSO or 0.1 μM CD had 20 calycal processes on average. Labeling intensity decreased with increasing drug concentration, becoming undetectable at 10 μM (Fig. 3C,D). The average number of calycal processes per cell with a detectable actin core was reduced to 17 at 1.0 μM and to zero at 10.0 μM CD.

Effect of CD on calycal process structure

When evaluated by TEM, calycal process structure appeared normal at 0.1 μM CD, whereas breakdown and collapse of calycal processes accompanied loss of the F-actin core at higher dosages of CD, as seen be Williams et al. (1988). In cross-sectional views, untreated and DMSO-treated calycal process profiles were circular to triangular, often conforming to the indentations of the rod OS incisures, and their membranes were distinct from the OS plasma membrane (Fig. 5A,D). The average number of calycal processes per rod photoreceptor was 20, as it was from fluorescence LSCM counts. The same was true for rods exposed to 0.1 μM CD (Fig. 5B,E). At 1.0 μM CD, a few calycal processes were misshapen and had occasionally

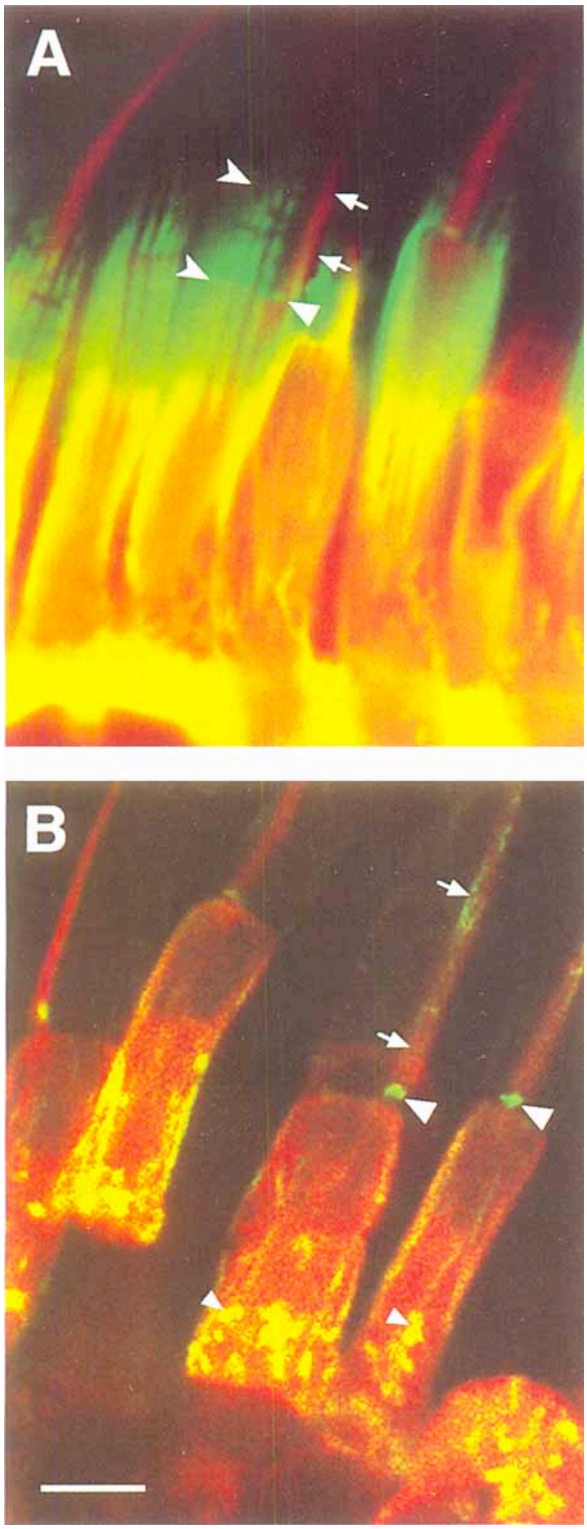

Fig. 2. Effect of 10 μM CD on actin filament organization. Double-label fluorescence laser scanning confocal microscopy (LSCM) images of longitudinally oriented *Xenopus laevis* photoreceptors. Rhodamine-tubulin immunofluorescence (red) marks the location of the ciliary microtubules (arrows), which run through the ciliary stalk and along one side of the OS. Fluorescein-phalloidin fluorescence (green) shows the location of F-actin. Areas containing both labels appear yellow. (**A**) Photoreceptors treated with 0.1% dimethyl sulfoxide (DMSO) in culture for 6 hours. Actin filaments are organized into cables that appear as intense lines and extend from the calycal processes (notched arrowheads) into the IS; a network, including some finer fibers, that appears as diffuse fluorescence in the IS; and a small network in the distal ciliary stalk that appears as a spot of fluorescence (arrowhead). (**B**) Photoreceptors treated with 10 μM CD for 6 hours. The fluorescein signal is intensified at the ciliary stalk (large arrowheads) and various foci (small arrowheads) in the IS, which have replaced the normal diffuse IS labeling, indicating aggregation of F-actin. Almost no phalloidin labeling of the calycal process-IS cables is detectable, indicating dispersal and/or contraction into the IS. Abbreviations as for Figure 1. Scale bar = 5 μm.

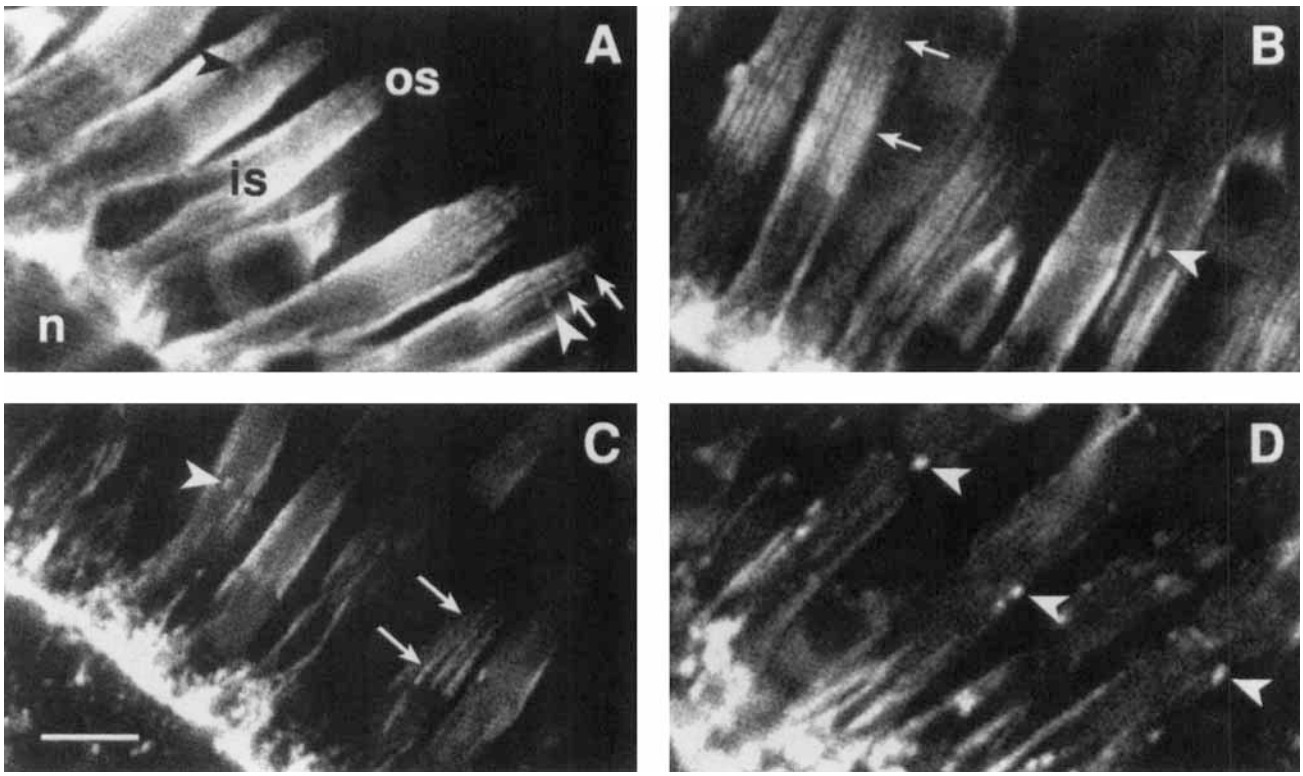

Fig. 3. Effect of varied concentrations of CD on actin filament organization. Fluorescence LSCM images of longitudinally oriented *Xenopus laevis* photoreceptors labeled with rhodamine-phalloidin. (**A**) Photoreceptors treated with DMSO alone for 6 hours. Calycal process (arrows)-inner segment (is) cables, a network in the IS and around the nucleus (n), and a discrete network in the ciliary stalk (arrowheads) at the base of the outer segment (os) are evident. This labeling pattern is the same as that seen in freshly dissected retinas (not shown). (**B–D**) Dose series: 0.1 μM CD (B), 1.0 μM CD (C), and 10.0 μM CD (D). Phalloidin labeling in the ciliary stalk (arrowheads) is progressively more intense at each higher dosage and changes in shape, becoming ovoid. (B) Labeling intensity of the calycal process-IS cables appears normal at 0.1 μM CD, although calycal processes (delimited by arrows) are elongated compared with those in A. (C and D) Increasingly bright, punctate labeling replaces the normally diffuse fluorescence in the IS and around the nucleus. Labeling of the calycal process-IS cables is diminished at 1.0 μM (arrows in C) and is nearly undetectable at 10.0 μM (D). A few small concentrations of fluorescence are present in the periphery where cables were located. Abbreviations as in Figures 1 and 2. Scale bar = 5 μm.

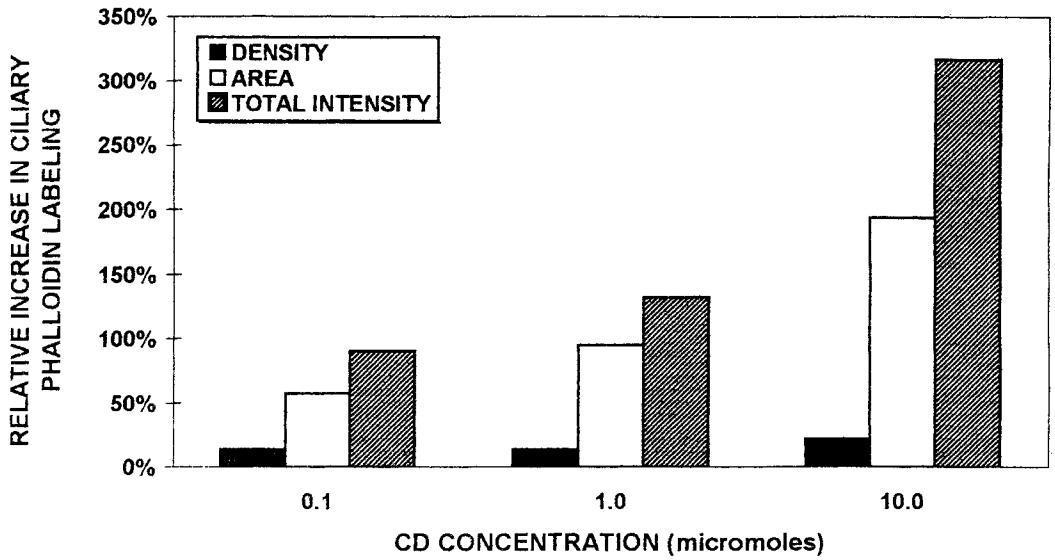

Fig. 4. Increase in the intensity of ciliary stalk phalloidin labeling in response to CD. Quantitation was performed on digitized LSCM images similar to those in Figure 3. After exposure to CD for 2 hours, the mean total intensity [mean (density × area)] of the fluorescent signal in the ciliary stalk was increased, relative to control values. The effect was greater at each higher dosage and was statistically significant at all concentrations ($P < 0.05$, 0.1 and 1.0 μM; $P < 0.01$, 10 μM). Values are averages of data from four retinas. Abbreviations as in Figures 1 and 2.

shortened or completely collapsed (not shown). The average number of calycal processes per rod photoreceptor at this dose was 18.5. At 10.0 μM CD, although the number of calycal processes decreased only to 16, many showed severe signs of breakdown, including irregular profile, reduced diameter, vesiculation, and infrequently, apparent fusion with the OS plasma membrane (Fig. 5C,F).

Association between effects on membrane morphogenesis and on the actin cytoskeleton

As delineated above, at 0.1 μM CD, disruption of OS disc membrane morphogenesis was associated with alteration of the actin network in the ciliary stalk, but not with dispersal of the actin core in the calycal processes and their structural breakdown, which occurred only at higher CD concentrations. This association was established not only for the average rod photoreceptor response, but in individual rods by both fluorescence LSCM and TEM. In rods treated with 0.1 μM CD and labeled with both biocytin plus fluorescein-avidin and rhodamine-phalloidin, a fluorescent sheet of ectopic disc membrane, an enlarged spot of fluorescence in the ciliary stalk, and normal calycal process fluorescence all could be found in all cells surveyed (not shown). In TEM cross-sections, ectopic disc membranes could be seen extending alongside rod OS that were surrounded by a full complement of intact calycal processes. These membranes appeared to have grown out between calycal processes and the OS, between adjacent calycal processes, exterior to calycal processes (Fig. 5E), or at the ciliary stalk (Fig. 5B) where calycal processes are not present.

Temperature response

A temperature shift of 10°C, from 17°C to 27°C, was used to accelerate the metabolic rate. The disc formation rate without and with CD treatment was measured to test for inhibition by the drug of the expected temperature-induced increase.

Effect of CD on disc formation rate at varied temperatures

In rod photoreceptors treated with DMSO alone, raising the temperature caused an increase in the rate of formation of new OS discs. This rate was quantified using the fluorescent band height assay described in Figure 1. When detected with fluorescent streptavidin, a stack of biocytin-labeled discs appears as a fluorescent band at the base of the OS. Because the mean height (distance along the long axis of the OS) of such a fluorescent band increases linearly for incubation times between 4 and 16 hours, it can serve as a measure of the rate of disc initiation or disc membrane assembly, as shown by Vaughan et al., (1989). Figure 6 shows examples of the bands of biocytin plus fluorescent streptavidin labeling in rods incubated for 12 hours at either 17°C (Fig. 6A) or 27°C (Fig. 6B). The mean fluorescent band height was 0.46 μm at 17°C and 1.28 μm at 27°C, a 2.8-fold increase in rate ($P < 0.005$, Student's t-test) (Fig. 7). This acceleration falls within the range of values obtained by other investigators for a 10°C temperature increase: 2-fold for 23–33°C in *Rana pipiens* tadpoles (Hollyfield et al., 1977), 3.5-fold for 16–26°C in *Rana pipiens* adults (Hollyfield, 1979), and 3-fold for 16–26°C in *Xenopus laevis* tadpoles (Hollyfield and Rayborn, 1982). Vaughan et al. (1989) has shown that DMSO treatment (0.25%) does not affect the rate of disc formation significantly. CD inhibited the response to temperature elevation. After pretreatment with 5 μM CD at 17°C, mean fluorescent band height was only slightly greater for rods shifted to the higher temperature: 0.33 μm at 27°C compared with 0.30 μm at 17°C (Fig. 6C,D; Fig. 7). In fact, both of these values were less than for the 17°C DMSO treatment. The difference between the normal response to a 10°C temperature increase and the response in the presence of CD, a 94% inhibition, was significant ($P < 0.025$), as evaluated by an analysis of variance test.

Effect of CD on disc membrane assembly rate at varied temperatures

There was no effect of CD on the rate at which disc membrane was assembled, in contrast to the above inhibition, which apparently represents a block of new disc initiation. The rate of membrane assembly in DMSO-treated rods also was measured as mean fluorescent band height after 12 hours, because membrane is added by lateral expansion of discs to a uniform size. This rate was 2.8 times greater at the higher temperature (see above; Fig. 7). Because membrane is added to the ectopically growing discs (Williams et al., 1988), the rate of membrane assembly in CD-treated rods was measured as the volume of the ectopic membrane sheets after 12 hours (Fig. 6E,F), as estimated by measurements of the mean width and length (Fig. 8) in combination with the mean fluorescent band height (Fig. 7). Although the width dimension was not significantly changed, the length dimension was 3.3 times greater ($P < 0.005$) at 27°C than at 17°C. Because the third dimension, the height of the stack of discs, differed only slightly, disc membrane was assembled at approximately a three-fold faster rate at the higher temperature. This increase is comparable to that measured in the absence of the drug.

Effect of CD on actin cytoskeleton at varied temperatures

The effect of CD at 5 μM (not shown) was similar to that at 10 μM (Fig. 3D). The only obvious difference between the pattern of fluorescent phalloidin labeling after CD treatment at 17°C and 27°C was an overall diminished intensity at the higher temperature, probably reflecting greater disassembly or dispersal. As noted above, CD altered the ciliary stalk actin network within 2 hours after addition to the culture medium. Hence, this network was disrupted before the temperature was raised at 2.5 hours after addition of the drug.

DISCUSSION

Effect of CD on actin filament organization

In a previous study, Williams et al. (1988) used CD to establish the actin dependence of photoreceptor disc membrane morphogenesis, but could not distinguish between the drug's action on the calycal process actin core and on the ciliary stalk actin network at the concentrations tested (5μM and 25 μM). We have tested a series of dosages starting with a lower concentration (0.1, 1.0, and 10.0 μM) in an attempt to identify the local actin filament array involved. The effects we observed were complex and dose dependent. For the actin structures in question, the effects became apparent at different concentrations.

Phalloidin staining (Figs. 2, 3) revealed loss of F-actin at some locations, in partial agreement with previous observa-

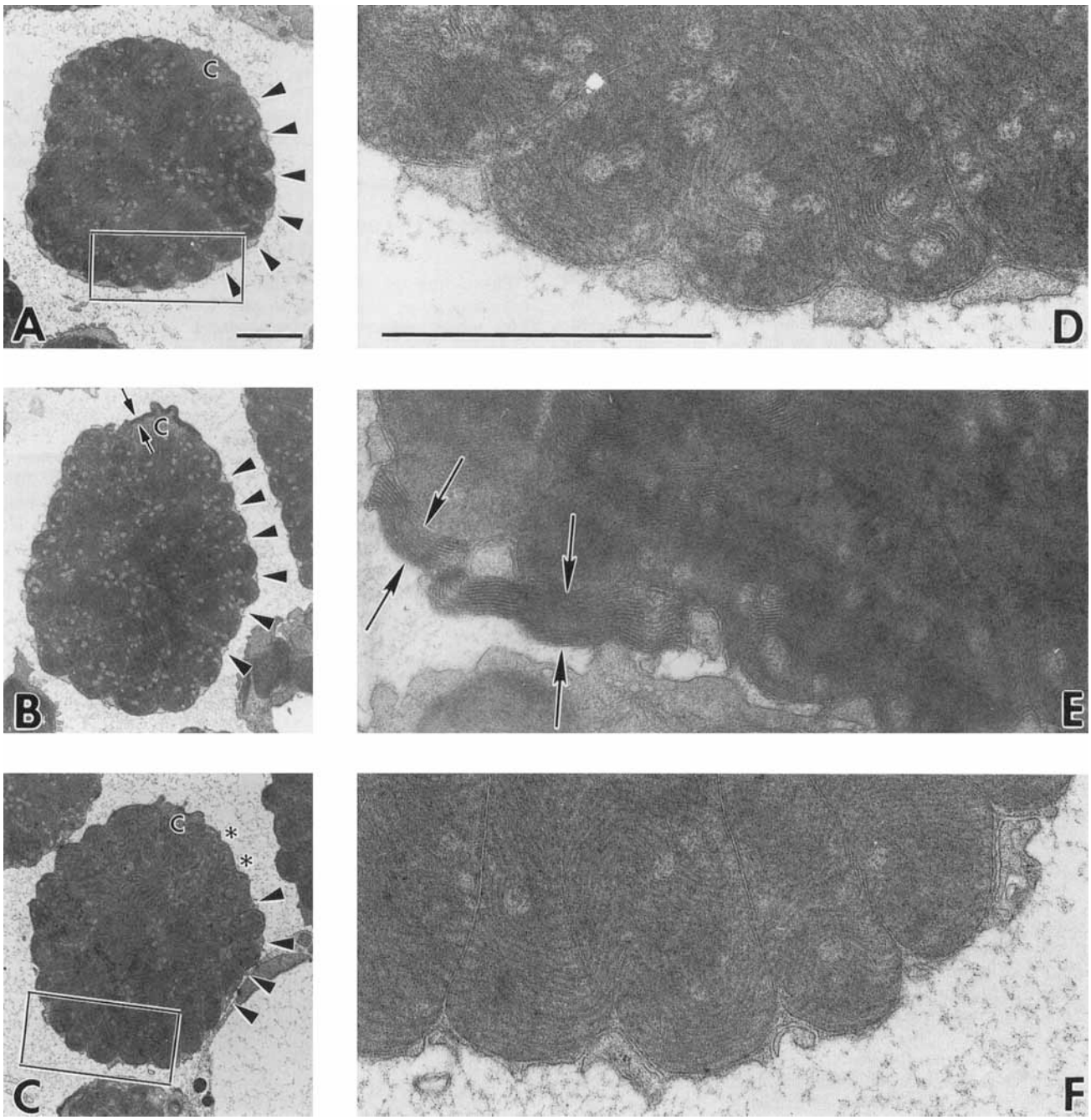

Fig. 5. Effect of CD on calycal process structure and disc membrane morphogenesis. Transmission electron microscopy (TEM) images of *Xenopus laevis* rod photoreceptors cut in cross-section through the OS near the base. (**A**) Rod treated with DMSO alone for 6 hours. Calycal processes (some marked by arrowheads), which project from the IS alongside the OS base, are located approximately at each disc incisure. None are present at the ciliary stalk (c). (**D**) Enlargement of the area outlined in A. The profile of calycal processes in retinas processed for TEM conform to the indentations to which they are adjacent. Their membranes are separate from the plasma membrane of the OS. This morphology also is seen in freshly dissected retinas (not shown). (**B**) Rod treated with 0.1 μM CD. Again, a calycal process is present at each incisure. Ectopic disc membranes are present alongside the ciliary stalk (apposing arrows). (**E**) Portion of another rod treated with 0.1 μM CD. A stack of ectopic disc membranes (apposing arrows) extends alongside the OS (orthogonal to the plane of section). The disc membranes are exterior to a calycal process. The calycal process profiles conform to the adjacent surface, similar to those in D, and their membranes are distinct from adjacent membrane. (**C**) Rod treated with 10 μM CD. At some incisures (asterisks), there is no calycal process visible. (**F**) Enlargement of the area outlined in C. These calycal processes show signs of collapse, including irregular shape and size, vesiculation, and possibly fusion with the OS plasma membrane. Scale bars = 2 μm.

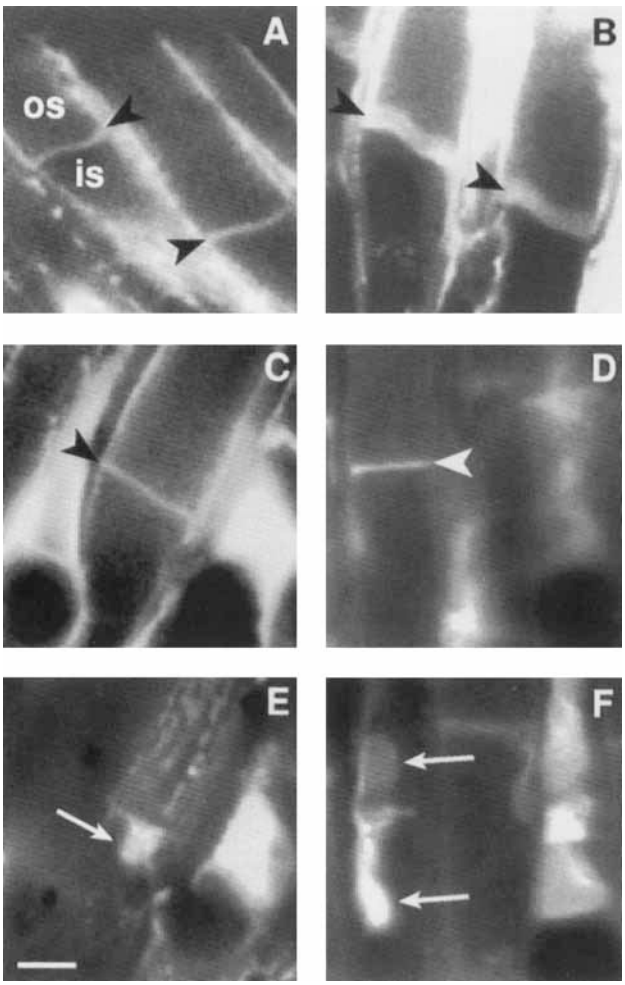

Fig. 6. Effect of CD on disc initiation and membrane assembly. Fluorescence LSCM images of fluorescent streptavidin bound to biocytin, which has accumulated in rod OS discs formed during incubation in medium containing the tracer (described in Fig. 1). (**A–D**) Optical sections collected at the center of longitudinally oriented *Xenopus laevis* rods. Labeled discs appear as a fluorescent band at the base of the outer segment (os; arrowheads). (**E, F**) Optical sections collected at the surface of the rods. After ectopic growth, labeled discs appear as a fluorescent sheet extending along the rod surface (arrows). (A and B) In DMSO-treated rods, the height of the fluorescent band is greater after 12 hours at 27°C (B) vs. 17°C (A), indicating accelerated disc initiation at the higher temperature. (C–F) In rods pretreated with 5 μM CD at 17°C, the heights of the fluorescent band either after a shift to 27°C for 12 hours in the presence of CD (D) or after continued incubation at 17°C (C) are similar. At the "is" surface of the same CD-treated rods, the ectopic membrane sheet extends over a greater area after incubation at 27°C (F) vs. 17°C (E), indicating accelerated membrane assembly at the higher temperature. Scale bar = 5 μm.

tions of Williams et al. (1988), and focal concentration at others, an effect not clearly seen by these investigators. A major difference in tissue preparation techniques is the most likely explanation for the difference in results. In the previous study, photoreceptor cells were isolated by enzymatic digestion before fixation. In this study, eyecups were fixed intact and then prepared for staining and viewing by sectioning with a Vibratome, a method likely to be more gentle. Cytochalasin-induced formation of focal concentrations of F-actin is a general phenomenon, which has been observed in a variety of plant and animal cells (Edmonds and Koenig, 1990 and references therein). These filamentous aggregates are postulated to arise by a two-part mechanism (Schliwa, 1982; Kolega et al., 1991). Solation of actin networks by CD produces short actin filaments that are still cross-linked. Disrupted networks or fragments thereof then actively condense. Therefore, it is likely that some of the apparent loss of F-actin from locations within the photoreceptor was a result of redistribution into foci. CD-induced contraction of individual stress fibers labeled by incorporation of fluorescent actin or myosin analogs has been followed in living fibroblasts (Kolega et al., 1991). As fibers shortened into bright foci, the fluorescence per length of fiber increased and the total fiber fluorescence decreased, indicating that both aggregation and actual loss, respectively, occur.

Foci formation appears to be an active process involving myosin-based contraction. It is prevented by inhibitors of energy metabolism, although network fragmentation is not, and requires ATP in permeabilized cells (Miranda et al., 1974; Bershadsky et al., 1980; Godman et al., 1980; Schliwa, 1982; Edmonds and Koenig, 1990). Myosin is concentrated in aggregates (Weber et al., 1976; Godman et al., 1980; Edmonds and Koenig, 1990; Kolega et al., 1991). Furthermore, CD can cause accelerated contraction of reconstituted actin gels, containing myosin and cross-linking proteins, in vitro (Janson et al., 1991). These findings illustrate part of the basis for the complexity of CD's effects in cells: the interaction of actin filaments with associated proteins, which organize and move filaments, contributes to the final effect. Myosin II has been immunolocalized in the ciliary network (Chaitin and Coelho, 1992; Williams et al., 1992) of rat rod photoreceptors and in the IS of rat rods (Drenckhahn and Groschel-Stewart, 1977; Williams et al., 1992) and photoreceptors of several species (Drenckhahn and Wagner, 1985). The ciliary network has been proposed to be contractile, based on the localization of myosin II (Chaitin and Coelho, 1992; Williams et al., 1992) and detection of myosin ATPase activity in isolated rat rod OS (Williams et al., 1992). In addition, α-actinin, an actin cross-linking protein, has been colocalized with actin in the ciliary network of rat photoreceptors (Arikawa and Williams, 1989) and in the IS of chicken photoreceptors (Drenckhahn and Wagner, 1985; Arikawa and Williams, 1991). These actin-associated proteins presumably are present at these same locations in frog rods. If so, the aggregation of F-actin in the photoreceptor ciliary stalk and at various foci in the IS in response to CD likely reflects excessive contraction of myosin-containing networks and possibly the IS cables, which in turn reflects fragmentation of filament arrays by CD.

The composition of the calycal process core of actin filaments is not fully characterized. Ultrastructurally, the core resembles that of intestinal epithelial microvilli; actin filaments are bundled and have their barbed ends embedded in a dense cap at the distal tip (Burnside, 1978; O'Connor and Burnside, 1981). However, not all of the actin-associated proteins in intestinal microvilli (Mooseker, 1985) are found in the calycal processes. Fimbrin—but not villin, myosin I, or ezrin—has been detected in the calycal processes (Hofer and Drenckhahn, 1993). The actin filament core in intestinal microvilli does not contain myosin II and is noncontractile (Mooseker, 1985). It is not known whether the same is true of the core in the calycal processes. If it is, it provides an explanation for the uniform decrease in F-actin concentration in each calycal process in response

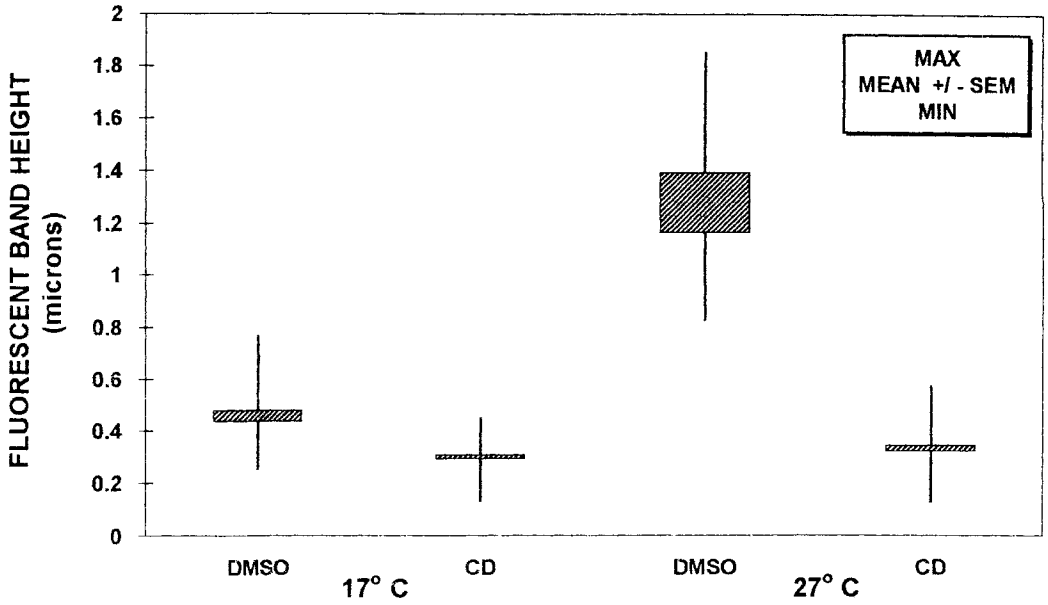

Fig. 7. Inhibition of temperature-induced increase in the rate of disc formation by CD. The rate of disc formation was measured as mean fluorescent band height after 12 hours incubation under the various conditions of temperature and CD treatment. Quantitation was performed on digitized LSCM images such as those in Fig. 6A–D. The 10°C temperature shift increased the rate 2.8-fold ($P < 0.005$) in the absence of CD, but only slightly after pretreatment with CD. Both the mean and the range of values at 27°C were reduced by CD treatment. The difference between the increase in the absence versus the presence of CD [(DMSO 27°C − DMSO 17°C) − (CD 27°C − CD 17°C)] is a 94% inhibition ($P < 0.025$; analysis of variance test). For DMSO treatment, the mean fluorescent band height also is a measure of the rate of disc membrane assembly. Data from eight retinas were pooled for each treatment. Bars represent ± 1 SEM; vertical lines represent the range. Abbreviations as for Figures 1 an 2.

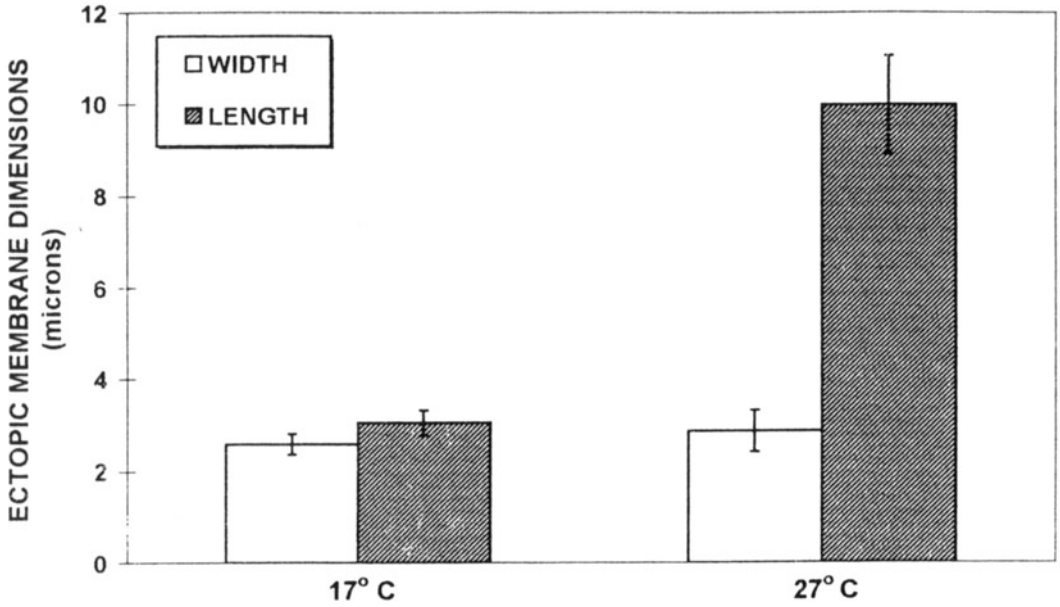

Fig. 8. Temperature-induced increase in the rate of disc membrane assembly in the presence of CD. The rate of disc membrane assembly was estimated from the mean width (1-D estimate of extent around rod circumference), length (extent along long axis of rod), and height (Fig. 7) dimensions of the ectopic membrane sheets after 12 hours incubation at either 17°D or 27°C. Quantitation was performed on digitized LSCM images such as those in Figure 6E,F. Only the mean length dimension differed substantially between the two temperatures. It, and therefore the membrane assembly rate, was increased 3.3-fold ($P < 0.005$) by the 10°C temperature shift. Values are averages of data from four retinas. Error bars represent ± 1 SEM. Abbreviations as in Figures 1 and 2.

to 1.0 and 10.0 μM CD. Even after a short (30 minutes), direct exposure of photoreceptors in isolated retinas to the drug (not shown), no concentration of F-actin within or near the base of the calycal processes was seen. Fragmentation of the calycal process core produced only dispersal of F-actin.

Both concentration of F-actin in the ciliary stalk and loss from the calycal processes increased progressively with increasing CD concentration (Fig. 3). For both actin filament arrays, a greater response could result from greater fragmentation. The degree of solation determines the degree of contraction of actin-based gels (Janson et al., 1991) and would be expected to determine the amount of dispersal of F-actin, in the form of gel fragments no longer attached to the array. The degree of solation at 0.1 μM may be very low, judging by the small average contraction response of the ciliary network, compared with that at 10.0 μM (Fig. 4), and retention of F-actin in the calycal processes (Fig. 3B). It is possible that part of the contraction response is caused by displacement of actin filament membrane attachments by capping of the barbed ends (reviewed by Cooper, 1987), which face the ciliary membrane in this array of roughly radially oriented filaments (Arikawa and Williams, 1989; Chaitin and Burnside, 1989). In this network, myosin is located centrally (Williams et al., 1992), within the ciliary microtubule array. In this arrangement, myosin activity would pull filaments in toward the center, and membrane attachments normally would provide resistance. Although the average percent increase in the density of fluorescent phalloidin labeling in the ciliary stalk was relatively small at each higher dose, the larger increase in the fluorescent area can be interpreted as substantial aggregation of filaments (Fig. 4). The labeling of this network normally is faint. Contraction would be expected to increase the fluorescent area because the normally sparse, and thus undetected, labeling at the periphery would reach the threshold of detection as filaments were pulled centrally, concentrating them.

Of the two local actin arrays whose disruption could interfere with disc membrane morphogenesis, only the ciliary stalk actin network appeared by light microscopy to be affected at 0.1 μM CD. Whereas F-actin concentration increased in the ciliary stalk at this dose, it remained normal in the calycal processes for up to 6 hours. Calycal processes maintained their normal length or, in some preparations, elongated. In other systems, stability of microvillus processes to treatment with even higher CD concentrations has been reported. In teleost rods, treatment with 10 μM CD for 1 hour did not remove the F-actin core of the calycal processes, whereas 0.1 μM was sufficient to block actin-dependent rod cell elongation (Pagh-Roehl et al., 1992). In epithelial cells, actin filaments were retained within microvilli after treatment with 1.0 μM CD in bladder epithelium (Franki et al., 1992), with 10 μM CD in an intestinal epithelial cell line (Jackman et al., 1994), and with 20 μM CD in intestinal epithelium (Madara et al., 1986), although other components of the actin cytoskeleton were disrupted in intestinal epithelial cells under the same conditions. Elongation of the calycal processes after CD treatment is not unexpected. Microvilli of intestinal and bladder epithelia have been observed to increase in length in response to certain concentrations of cytochalasin (Burgess and Grey, 1974; Franki et al., 1992). In addition, calycal process length varies under other conditions. It has been shown to change inversely with myoid contraction and elongation in teleost rods (Pagh-Roehl et al., 1992).

A difference in the composition of the arrays could underlie the apparent difference in sensitivity to CD. In addition to being noncontractile, the microvillar core of actin filaments is highly cross-linked (Mooseker, 1985). As this appears to be true of calycal processes (Burnside, 1978; Hofer and Drenckhahn, 1993), contraction would not be expected to occur in response to capping and fragmentation by CD, and dispersal of the fragmented array would be hindered by the cross-linking. Disruption by CD would not be immediately evident. Therefore, there is a possibility that the calycal processes, although they exhibited no signs of collapse at 0.1 μM, were less rigid. Although there may not have been a difference in sensitivity to CD in terms of the initial effects of capping and fragmentation, there was a difference in terms of the final effect. Aggregation of ciliary stalk F-actin provided evidence of structural alteration, from which we assume that the function of this network was impaired at 0.1 μM CD. We speculate that the proposed function of the calycal processes as a signal for termination of disc membrane outgrowth was not impaired at this dose, however, as it probably would involve contact inhibition rather than presentation of a physical barrier.

Other populations of actin filaments also could be important to OS disc morphogenesis, including filaments seen in rat rods that extend longitudinally within the ciliary stalk (Arikawa and Williams, 1989) and arrays and cables within the IS (Drenckhahn and Wagner, 1985; Nagle et al., 1986; Vaughan and Fisher, 1987). Longitudinally oriented actin filaments within the ciliary stalk could participate in apical displacement of discs, which presumably must precede initiation of each new ciliary membrane evagination. We did not specifically detect such a population of filaments within the ciliary stalk by phalloidin labeling. Vesicle transport can occur along actin filaments (Kuznetsov et al., 1992), and IS filaments could be involved in the delivery of structural components or regulatory molecules to the ciliary stalk (Deretic et al., 1995). We were not able to pinpoint any alterations in IS phalloidin labeling at 0.1 μM CD. Hence, effects of CD via these components of the actin cytoskeleton can neither be supported nor rejected by this study.

Effect of CD on membrane morphogenesis

CD induced abnormal disc membrane outgrowth at a concentration (0.1 μM) that did not remove the actin core in the calycal processes, but did disrupt the actin filament network in the ciliary stalk. These effects of CD were examined separately as sample averages and together in individual cells. At 0.1 μM, ectopic disc membranes were detected by fluorescence LSCM in only 21% of rod photoreceptors, probably because not all rods are affected completely at this dose. Support for this reasoning comes from the ranges of the total intensity values for ciliary stalk phalloidin labeling measured after treatment with DMSO or 0.1 μM CD. The ranges overlap, suggesting that the ciliary actin network is not disrupted in all rods at 0.1 μM; hence, the function of the network is at least partially retained in some fraction of the rods. It is not clear why ectopic discs were detected in a greater proportion of rods at 10.0 μM than at 1.0 μM CD. This characteristic made examination of individual rods important. In cells surveyed either by double-label fluorescence LSCM or by TEM, the presence of ectopic disc membranes always was associated with an enlarged concentration of fluorescence in the ciliary stalk and normal calycal process fluorescence or with normal calycal process ultrastructure. Thus, CD most likely acts on F-actin in the ciliary stalk to perturb disc morphogenesis. This conclusion provides support for the model proposed by Williams et al. (1988) in which the ciliary actin network is involved in the initiation of membrane evagination.

Consistent with this hypothesis, fewer new discs than normal are generated in the presence of CD. In the study by Williams et al. (1988), nascent discs were radiolabeled by incorporation of proteins containing ^{3}H-leucine. When viewed by autoradiography, the band of radiolabel at the OS base was substantially shorter in rods treated with CD than in rods treated with DMSO alone. Vaughan et al. (1989) labeled nascent discs with the fluorescent dye Lucifer yellow. They measured a significant reduction in mean fluorescent band height with CD. However, these observations do not reveal whether the effect of the drug on disc initiation is direct or indirect.

To answer the question of which morphogenic step CD inhibits, we took advantage of the proportional relationship between the rate of disc formation and temperature (Hollyfield et al., 1977; Hollyfield, 1979; Hollyfield and Rayborn, 1982; Kaplan, 1984). If it is the initiation step that is inhibited, then temperature elevation should cause no increase in the rate of disc formation in the presence of CD. If not, temperature elevation could cause a partial increase because initiation is possible and membrane assembly would be more rapid, although some step is abnormal. For DMSO-treated rods, we calculated a nearly three-fold increase in the average rate of disc formation for a 10°C rise in temperature from measurements obtained using the fluorescent band height assay (Fig. 7). Pretreatment with CD caused a 94% inhibition of this temperature-induced increase. This nearly complete inhibition is evidence for a direct effect of CD on the initiation step.

Another factor that could contribute to the greatly decreased temperature response is a reduction of the rate of membrane assembly by CD. Therefore, it was important to determine whether the disc membrane assembly rate in CD-treated rods showed the normal temperature-induced increase before accepting the above conclusion. The rate increase in the presence of the drug, calculated from measurements of the volume of ectopic membrane assembled, was the full response seen in its absence, calculated from fluorescent band height measurements. The 10°C rise in temperature caused approximately a three-fold acceleration of disc membrane assembly in both CD-treated rods and control rods (Figs. 7,8), upholding the conclusion that CD directly affects the initiation step. This result expands on the autoradiographic demonstration by Williams et al. (1988) that transport and assembly of disc membrane components persist in the presence of CD. Newly synthesized proteins, radiolabeled with ^{3}H-leucine, were incorporated into the ectopic disc membranes. The initiation and membrane assembly steps can be uncoupled. It is not clear why outgrowth of existing discs, potentially an actin-mediated process, is not sensitive to CD.

It is possible that blocking of another step in the disc morphogenesis process could indirectly slow the creation of new discs. Several alternate possibilities exist. Although membrane assembly continues, these possibilities could involve disruption of the delivery of certain structural components or regulatory molecules from the IS by the action of CD on IS actin filaments. As discussed above, we did not observe any effects of 0.1 μM CD on phalloidin labeling in the IS. First, CD could prevent response to a signal, for instance, calycal process contact inhibition, to halt outgrowth of the disc-face membranes. Second, it could block the outgrowth of rim-plasma membrane, which seals the disc. In both of these cases, disc growth could continue unregulated, and excessive growth of preexisting discs would divert material from new sites of disc formation. The initiation of ciliary membrane evagination would still be possible, and some new discs could be added. The nearly complete inhibition of the temperature-induced acceleration of the disc formation rate argues that CD effects on the control of disc size are secondary or, because they are not ruled out, perhaps coincident. The second alternative seems unlikely for an additional reason—completing disc closure does not appear to be necessary for control of disc size. Indeed, in cone photoreceptors, rim closure is only partial. Furthermore, in rods, ectopic disc membranes have not been detected when the number of immature, that is, open discs is maximal. This occurs when disc addition is stimulated by light or temperature. The increase in disc formation rate is correlated with an increase in the number of open discs, indicating that rim closure does not keep pace with growth of the disc-face membranes (Besharse et al., 1977; Hollyfield and Rayborn, 1982). These two possibilities could involve putative F-actin arrays in the periphery of the expanding disc membrane evagination or in the rim-plasma membrane projections, respectively, that were not detected by our methods.

A third possibility is that CD blocks apical displacement of discs. This could prevent the construction of new sites of ciliary membrane evagination. We cannot distinguish between this indirect effect of CD and a direct effect on disc initiation from the temperature response or phalloidin labeling data. In both cases, CD would be expected to block new disc initiation completely. The actin filaments in the ciliary network contact several of the newest discs and thus could be involved in their displacement. Involvement of the same actin network would link these effects. The large size of maturing and completed discs would seem to require additional cytoskeletal or molecular motor involvement. Phalloidin labeling in other regions of the OS was not detected in this study.

The conclusions from our examination of CD's action on specific actin filament arrays and on a specific step in the disc morphogenesis process imply an essential role for the ciliary stalk actin network in the generation of new OS discs. Disruption of this network is linked to abnormal disc morphogenesis, and CD nearly completely inhibits new disc initiation. CD most likely affects the initiation step by blocking the initiation of ciliary membrane evagination and/or the apical displacement of discs. Two characteristics of the photoreceptor ciliary actin network fit well with this role. First, the network appears during photoreceptor maturation just before the first discs form. Chaitin et al. (1988) has immunolocalized actin in the distal portion of mouse photoreceptor cilia at this stage. Actin was present only in those cilia that displayed a swelling of the distal portion, a morphological feature thought to be a precursor to the initiation of disc formation (Olney, 1968). Myosin subfragment-1 decoration has revealed actin filaments organized in a network (Chaitin, 1991; Obata and Usukura, 1992) similar to that seen in the adult rodent (Arikawa and Williams, 1989; Chaitin and Burnside, 1989). Second, the network seemingly is unique to photoreceptor cilia, as is membranous disc formation. No equivalent contractile network has been found in motile cilia or flagella. They have been shown to contain actin, but actin in filamentous form has not been detected by either NBD-phallacidin staining or myosin subfragment-1 decoration (Virtanen et al., 1984; Detmers et al., 1985; Chailley et al., 1986; Sandoz et al., 1988). Myosin and tropomyosin immunolabeling

have been detected, but only in the proximal portion and the basal bodies of cilia (Gordon et al., 1980; Sandoz et al., 1982; Virtanen et al., 1984) or in the neck region of flagella (Yagi and Paranko, 1992). Hence, in the cilia of oviduct epithelium (Sandoz et al., 1982) and in sperm flagella (Yagi and Paranko, 1992), where actin and myosin or tropomyosin were observed to colocalize by immunocytochemistry, the location does not correspond to that of the photoreceptor ciliary network. Thus, the evidence suggests that vertebrate photoreceptors have evolved a mechanism that uses the functional properties of F-actin in a unique way in the cilium compared with other ciliated cell types. This mechanism is the key to their ability to elaborate the membranous discs that form the light-sensitive OS.

ACKNOWLEDGMENTS

We are grateful to Mr. Scott Gaitin for technical assistance, to Dr. Michael Klymkowsky for the gift of the antibody to β-tubulin, to Dr. Leslie Wilson for use of the Hamamatsu DV 3000 image processor and the image analysis system, to Optronics Engineering, Inc. for use of the TEC-470 CCD camera, to Ms. Maura Jess and Mr. Dave Folks for assistance with dye sublimation printing, to Ms. Donna Medrano for expert photographic processing, to Mr. Mark Wendell and Ms. Maura Jess for the computer-generated diagrams, and to Dr. Pat Ross for advice on statistics. This research was supported by National Institutes of Health grants EY-07191 to B.M. and EY-00888 to S.K.F. and by two Sigma Xi Grants-in-Aid of Research from the National Academy of Sciences to I.L.H.

LITERATURE CITED

Arikawa, K., and D.S. Williams (1989) Organization of actin filaments and immunocolocalization of alpha-actinin in the connecting cilium of rat photoreceptors. J. Comp. Neurol. *288:*640–646.

Arikawa, K., and D.S. Williams (1991) Alpha-actinin and actin in the outer retina: A double immunoelectron microscopic study. Cell Motil. Cytoskeleton *18:*15–25.

Bershadsky, A.D., V.I. Gelfand, T.M. Svitkina, and I.S. Tint (1980) Destruction of microfilament bundles in mouse embryo fibroblasts treated with inhibitors of energy metabolism. Exp. Cell Res. *127:*421–429.

Besharse, J.C. (1980) Light and membrane biogenesis in rod photoreceptors of vertebrates. In T.P. Williams and B.N. Baker (eds): The Effects of Constant Light on Visual Processes. New York: NY: Plenum Press, pp. 409–431.

Besharse, J.C., and D.A. Dunis (1983) Rod photoreceptor disc shedding in eye cups: Relationship to bicarbonate and amino acids. Exp. Eye Res. *36:*567–580.

Besharse, J.C., J.G. Hollyfield, and M.E. Rayborn (1977) Turnover of rod photoreceptor outer segments. II. Membrane addition and loss in relationship to light. J. Cell Biol. *75:*507–527.

Boisvieux-Ulrich, E., M.C. Laine, and D. Sandoz (1990) Cytochalasin D inhibits basal body migration and ciliary elongation in quail oviduct epithelium. Cell Tissue Res. *259:*443–454.

Burgess, D.R., and R.D. Grey (1974) Alterations in morphology of developing microvilli elicited by cytochalasin B. Studies of embryonic chick intestine in organ culture. J. Cell Biol. *62:*566–574.

Burnside, B. (1978) Thin (actin) and thick (myosinlike) filaments in cone contraction in the teleost retina. J. Cell Biol. *78:*227–246.

Chailley, B., K. Bork, P. Gounon, and D. Sandoz (1986) Immunological detection of actin in isolated cilia from quail oviduct. Biol. Cell *58:*43–52.

Chaitin, M.H. (1991) Actin filaments in the photoreceptor cilium of the rds mutant mouse. Exp. Eye Res. *53:*107–113.

Chaitin, M.H., and D. Bok (1986) Immunoferritin localization of actin in retinal photoreceptors. Invest. Ophthalmol. Vis. Sci. *27:*1764–1767.

Chaitin, M.H., and B. Burnside (1989) Actin filament polarity at the site of rod outer segment disk morphogenesis. Invest. Ophthalmol. Vis. Sci. *30:*2461–2469.

Chaitin, M.H., and N. Coelho (1992) Immunogold localization of myosin in the photoreceptor cilium. Invest. Ophthalmol. Vis. Sci. *33:*3103–3108.

Chaitin, M.H., B.G. Schneider, M.O. Hall, and D.S. Papermaster (1984) Actin in the photoreceptor connecting cilium: Immunocytochemical localization to the site of outer segment disk formation. J. Cell Biol. *99:*239–247.

Chaitin, M.H., R.B. Carlsen, and G.J. Samara (1988) Immunogold localization of actin in developing photoreceptor cilia of normal and rds mutant mice. Exp. Eye Res. *47:*437–446.

Chu, D.T., and M.W. Klymkowsky (1989) The appearance of acetylated a-tubulin during early development and cell differentiation in Xenopus. Dev. Biol. *136:*104–117.

Cooper, J.A. (1987) Effects of cytochalasin and phalloidin on actin. J. Cell Biol. *105:*1473–1478.

Deretic, D., L.A. Huber, N. Ransom, M. Mancini, K. Simons, and D.S. Papermaster (1995) rab8 in retinal photoreceptors may participate in rhodopsin transport and in rod outer segment disk morphogenesis. J. Cell Sci. *108:*215–224.

Detmers, P.A., J.M. Carboni, and J. Condeelis (1985) Localization of actin in Chlamydomonas using antiactin and NBD-phallacidin. Cell Motil. *5:*415–430.

Drenckhahn, D., and U. Groschel-Stewart (1977) Localization of myosin and actin in ocular nonmuscle cells. Cell Tissue Res. *181:*493–503.

Drenckhahn, D., and H.-J. Wagner (1985) Relation of retinomotor responses and contractile proteins in vertebrate retinas. Eur. J. Cell Biol. *37:*156–168.

Edmonds, B.T., and E. Koenig (1990) ATP and calmodulin dependent actomyosin aggregates induced by cytochalasin D in goldfish retinal ganglion cell axons in vitro. J. Neurobiol. *21:*555–566.

Franki, N., G. Ding, Y. Gao, and R.M. Hays (1992) Effects of cytochalasin D on the actin cytoskeleton of the toad bladder epithelial cell. Am. J. Physiol. *263:*C995–C1000.

Godman, G., B. Woda, and R. Kolberg (1980) Redistribution of contractile and cytoskeletal components induced by cytochalasin. I. In Hmf cells, a nontransformed fibroblastoid line. Eur. J. Cell Biol. *22:*733–744.

Gordon, R.E., B.P. Lane, and F. Miller (1980) Identification of contractile proteins in basal bodies of ciliated tracheal epithelial cells. J. Histochem. Cytochem. *28:*1189–1197.

Hale, I.L., and B. Matsumoto (1993) Resolution of subcellular detail in thick tissue sections: Immunohistochemical preparation and fluorescence confocal microscopy. Methods Cell Biol. *38:*289–324.

Hofer, D., and D. Drenckhahn (1993) Molecular heterogeneity of the actin filament cytoskeleton associated with microvilli of photoreceptors, Muller's glial cells and pigment epithelial cells of the retina. Histochemistry *99:*29–35.

Hollyfield, J.G. (1979) Membrane addition to photoreceptor outer segments: Progressive reduction in the stimulatory effect of light with increased temperature. Invest. Ophthalmol. Vis. Sci. *18:*977–981.

Hollyfield, J.G., and M.E. Rayborn (1982) Membrane assembly in photoreceptor outer segments: Progressive increase in "open" basal discs with increased temperature. Exp. Eye Res. *34:*115–119.

Hollyfield, J.G., J.C. Besharse, and M.E. Rayborn (1977) Turnover of rod photoreceptor outer segments. I. Membrane addition and loss in relationship to temperature. J. Cell Biol. *75:*490–506.

Jackman, M.R., W. Shurety, J.A. Ellis, and J.P. Luzio (1994) Inhibition of apical but not basolateral endocytosis of ricin and folate in Caco-2 cells by cytochalasin D. J. Cell Sci. *107:*2547–2556.

Janson, L.W., J. Kolega, and D.L. Taylor (1991) Modulation of contraction by gelation/solation in a reconstituted motile model. J. Cell Biol. *114:*1005–1015.

Kaplan, M.W. (1984) Shedding is correlated with disk membrane axial position rather than disk age in Xenopus laevis rod outer segments. Vision Res. *24:*1163–1168.

Kaplan, M.W., D.A. Robinson, and L.D. Larsen (1982) Rod outer segment birefringence bands record daily disc membrane synthesis. Vision Res. *22:*1119–1121.

Kolega, J., L.W. Janson, and D.L. Taylor (1991) The role of solation-contraction coupling in regulating stress fiber actin dynamics in nonmuscle cells. J. Cell Biol. *114:*993–1003.

Kuznetsov, S.A., G.M. Langford, and D.G. Weiss (1992) Actin-dependent organelle movement in squid axoplasm. Nature *356:*722–725.

Lankford, K.L., and P.C. Letourneau (1991) Roles of actin filaments and three second-messenger systems in short-term regulation of chick dorsal root ganglion neurite outgrowth. Cell Motil. Cytoskeleton *20:*7–29.

Laties, A.M., D. Bok, and P.A. Liebman (1976) Procion yellow: A marker for outer segment disc patency and rod renewal. Exp. Eye Res. *23:*139–143.

Madara, J.L., D. Barenberg, and S. Carlson (1986) Effects of cytochalasin D on occluding junctions of intestinal absorptive cells: Further evidence that the cytoskeleton may influence paracellular permeability and junctional charge selectivity. J. Cell Biol. *102:*2125–2136.

Marsh, L., and P.C. Letourneau (1984) Growth of neurites without filopodial or lamellipodial activity in the presence of cytochalasin B. J. Cell Biol. *99:*2041–2047.

Matsumoto, B., and J.C. Besharse (1985) Light and temperature modulated staining of the rod outer segment distal tips with Lucifer yellow: A fluorescence microscope study. Invest. Ophthalmol. Vis. Sci. *26:*628–635.

Matsumoto, B., and I.L. Hale (1993) Preparation of retinas for studying photoreceptors with confocal microscopy. Methods Neurosci. *15:*54–71.

Miranda, A.F., G.C. Godman, A.D. Deitch, and S.W. Tanenbaum (1974) Action of cytochalasin D on cells of established lines. I. Early events. J. Cell Biol. *61:*481–500.

Mooseker, M.S. (1985) Organization, chemistry, and assembly of the cytoskeletal apparatus of the intestinal brush border. Ann. Rev. Cell Biol. *1:*209–241.

Muller, L.L., and T.J. Jacks (1975) Rapid chemical dehydration of samples for electron microscopic examinations. J. Histochem. Cytochem. *23:*107–110.

Nagle, B.W., C. Okamoto, B. Taggart, and B. Burnside (1986) The teleost cone cytoskeleton: Localization of actin, microtubules, and intermediate filaments. Invest. Ophthalmol. Vis. Sci. *27:*689–701.

Obata, S., and J. Usukura (1992) Morphogenesis of the photoreceptor outer segment during postnatal development in the mouse (BALB/c) retina. Cell Tissue Res. *269:*39–48.

O'Connor, P., and B. Burnside (1981) Actin-dependent cell elongation in teleost retinal rods: Requirement for actin filament assembly. J. Cell Biol. *89:*517–524.

Olney, J.W. (1968) An electron microscopic study of synapse formation, receptor outer segment development, and other aspects of developing mouse retina. Invest. Ophthalmol. Vis. Sci. *7:*250–268.

Pagh-Roehl, K., J. Brandenburger, E. Wang, and B. Burnside (1992) Actin-dependent myoid elongation in teleost rod inner/outer segments occurs in the absence of net actin polymerization. Cell Motil. Cytoskeleton *21:*235–251.

Sampath, P., and T.D. Pollard (1991) Effects of cytochalasin, phalloidin, and pH on the elongation of actin filaments. Biochemisty *30:*1973–1980.

Sandoz, D., P. Gounon, E. Karsenti, and M. Sauron (1982) Immunocytochemical localization of tubulin, actin, and myosin in axonemes of ciliated cells from quail oviduct. Proc. Natl. Acad. Sci. USA *79:*3198–3202.

Sandoz, D., B. Chailley, E. Boisvieux-Ulrich, M. Lemullois, M. Laine, and G. Bautista-Harris (1988) Organization and functions of cytoskeleton in metazoan ciliated cells. Biol. Cell *63:*183–193.

Schliwa, M. (1982) Action of cytochalasin D on cytoskeletal networks. J. Cell Biol. *92:*79–91.

Schliwa, M., and J. van Blerkom (1981) Structural interaction of cytoskeletal components. J. Cell Biol. *90:*222–235.

Spurr, A.R. (1969) A low-viscosity epoxy resin embedding medium for electron microscopy. J. Ultrastruct. Mol. Struct. Res. *26:*31–43.

Steinberg, R.H., S.K. Fisher, and D.H. Anderson (1980) Disc morphogenesis in vertebrate photoreceptors. J. Comp. Neurol. *190:*501–519.

Tilney, L.G., and S. Inoué (1982) Acrosomal reaction of Thyone sperm. II. The kinetics and possible mechanism of acrosomal process elongation. J. Cell Biol. *93:*820–827.

Vaughan, D.K., and S.K. Fisher (1987) The distribution of F-actin in cells isolated from vertebrate retinas. Exp. Eye Res. *44:*393–406.

Vaughan, D.K., and S.K. Fisher (1989) Cytochalasin D disrupts outer segment disc morphogenesis in situ in rabbit retina. Invest. Ophthalmol. Vis. Sci. *30:*339–342.

Vaughan, D.K., S.K. Fisher, S.A. Bernstein, I.L. Hale, K.A. Linberg, and B. Matsumoto (1989) Evidence that microtubules do not mediate opsin vesicle transport in photoreceptors. J. Cell Biol. *109:*3053–3062.

Virtanen, I., R.A. Badley, R. Paasivuo, and V.P. Lehto (1984) Distinct cytoskeletal domains revealed in sperm cells. J. Cell Biol. *99:*1083–1091.

Weber, K., Rathke, P.C., Osborn, M., and W.W. Franke (1976) Distribution of actin and tubulin in cells and in glycerinated cell models after treatment with cytochalasin B (CB). Exp. Cell Res. *102:*285–297.

Wessells, N.K., B.S. Spooner, J.F. Ash, M.O. Bradley, M.A. Luduena, E. Taylor, J.T. Wrenn, and K.M. Yamada (1971) Microfilaments in cellular and developmental processes. Science *171:*135–143.

Williams, D.S., K.A. Linberg, D.K. Vaughan, R.N. Fariss, and S.K. Fisher (1988) Disruption of microfilament organization and deregulation of disk morphogenesis by cytochalasin D in rod and cone photoreceptors. J. Comp. Neurol. *272:*161–176.

Williams, D.S., M.A. Hallett, and K. Arikawa (1992) Association of myosin with the connecting cilium of rod photoreceptors. J. Cell Sci. *103:*183–190.

Wrenn, J.T., and N.K. Wessells (1970) Cytochalasin B: Effects upon microfilaments involved in morphogenesis of estrogen-induced glands of oviduct. Proc. Natl. Acad. Sci. USA *66:*904–908.

Wulf, E., A. Deboben, F.A. Bautz, H. Faulstich, and T. Wieland (1979) Fluorescent phallotoxin, a tool for the visualization of cellular actin. Proc. Natl. Acad. Sci. USA *76:*4498–4502.

Yagi, A., and J. Paranko (1992) Localization of actin, alpha-actinin, and tropomyosin in bovine spermatozoa and epididymal epithelium. Anat. Rec. *233:*61–74.

Yahara, I., F. Harada, S. Sekita, K. Yoshihira, and S. Natori (1982) Correlation between effects of 24 different cytochalasins on cellular structures and cellular events and those on actin in vitro. J. Cell Biol. *92:*69–78.

Young, R.W., and B. Droz (1968) The renewal of protein in retinal rods and cones. J. Cell Biol. *39:*169–184.

Young, R.W., and D. Bok (1969) Participation of the retinal pigment epithelium in the rod outer segment renewal process. J. Cell Biol. *42:*392–403.